Proceedings Paper:

Li, X., Liu, Y., Yang, L. et al. (2 more authors) (2021) Enhanced fixed-interval smoothing for Markovian switching systems. In: de Villiers, P., de Waal, A. and Gustafsson, F., (eds.) 2021 IEEE 24th International Conference on Information Fusion (FUSION). 24th International Conference on Information Fusion (Fusion 2021), 01-04 Nov 2021, Sun City, South Africa. IEEE (Institute of Electrical and Electronics Engineers) . ISBN 9781665414272

Enhanced Fixed-Interval Smoothing for Markovian Switching Systems

Xi Li[1], Yi Liu[2], Le Yang[2*], Lyudmila Mihaylova[3], Bing Deng[4]
1. State Key Lab of Complex Electromagnetic Environment Effects on Electronics and Information Systems, National University of Defense Technology, Changsha China
2. Department of Electrical and Computer Engineering, University of Canterbury, Christchurch NZ
3. Department of Automatic Control and System Engineering, University of Sheffield, Sheffield UK
4. National Key Lab of Science and Technology on Blind Signal Processing, Chengdu, China
*: Corresponding author, le.yang@canterbury.ac.nz

***Abstract*—This paper considers the problem of fixed-interval smoothing for Markovian switching systems with multiple linear state-space models. An enhanced algorithm that is capable of accurately approximating the Bayesian optimal smoother is proposed. It utilizes the exact expression for the quotient of two Gaussian densities to help solve the backward-time recursive equations of Bayesian smoothing, and computes the joint posterior of the state vector and model index. The proposed algorithm only involves the approximation of each model-matched state posterior, which is a Gaussian mixture, with a single Gaussian density for maintaining computational tractability in retrodiction. The validity of the newly developed smoother is verified using a simulated maneuvering target tracking task.**

I. Introduction

Estimating the state of a dynamic system at a particular time can be carried out through utilizing either the measurements collected before and up to that time, or the measurements received before and beyond that time. The former approach is commonly referred to as *filtering* [1], while the latter is called *smoothing* or *retrodiction* [2], [3]. For linear state-space models with white Gaussian noise, the Rauch-Tung-Striebel (RTS) smoother [4], also known as the Kalman smoother, provides the optimal smoothing solution in closed form.

In practice, the system state may be subject to abrupt changes due to e.g., load disturbances, additive faults [5], [6] and target maneuvering [7]. This type of impulsive disturbances often leads to jumps in the state and they cannot be modeled by Gaussian process noise effectively. In [5], [6], smoothing in the presence of state jumps is accomplished by solving a convex optimization problem with sum-of-norms regularization to make use of the sparsity of the disturbances. Multiple model smoothing is another popular technique to handle the abrupt changes. It employs a set of candidate state-space models and finds the state estimates by combining the model-conditioned smoothed state posteriors [8].

We shall consider in this paper fixed-interval multiple model smoothing. Here, the system of interest is assumed to switch among a prefixed set of candidate state-space models. Its states over a time window are identified using *all* the measurements collected within the time window. For this problem, there exist a few suboptimal methods in literature. They are approximations to the Bayesian optimal solution, which is computationally intractable due to the number of hypotheses growing exponentially with respect to the window length. These techniques have been applied to help extract accurate tracks in multiple hypothesis tracking (MHT) [9]. They were also shown to be able to improve the performance of sensor registration and fusion in radar networks [10], articulatory inversion [11], maneuvering target tracking [12]–[14] and air traffic control (ATC) trajectory reconstruction [15].

Among the existing multiple model smoothers, the two-filter approach [16] finds the smoothed state estimates through combining the output of a forward-time interacting multiple model (IMM) filter and a backward-time IMM filter. This method is in fact an extension of the Frazer-Potter optimal linear smoother [17], [18] developed for the case with a single state-space model. It uses the normalizable state posterior provided by the backward-time filter to replace the non-normalizable measurement likelihood, which may be a poor approximation [3], [19]. In [20], the system states over a few consecutive time instants are collected to form an augmented state so that the forward-time IMM filter can be used to achieve multiple model smoothing. This approach assumes that there are no model switchings within the time span of the augmented state.

In [9], a generalized pseudo-Bayesian of order 2 (GPB2)-type multiple model smoother was proposed. To bypass the difficulty in evaluating the integral required for retrodiction, it assumes that smoothed state estimates are sufficiently accurate and can be considered noise-free. This could lead to performance degradation under relatively large noise levels. In [21], an IMM-type smoother was developed. Besides the use of sufficient statistics to replace measurements when computing the posterior probability of the model index, several strong assumptions on state-space models are also introduced [22]. In [22]–[24], the proposed algorithm combines the output of a forward-time IMM filter and backward-time RTS smoothers to carry out state smoothing. Laplace approximation is utilized in its model interaction step to approximate the non-normalizable quotient of two Gaussian densities. Its performance is close to that of the two-filter approach but it does outperform the methods in [9] and [21]. Recently, based on the framework of [22], the problem of multiple model smoothing when the process and measurement noises are both non-Gaussian was considered in [25].

The main contributions of this paper are as follows. 1) We develop an enhanced fixed-interval smoother for Markovian switching systems under Gaussian noises. The smoothed *joint* posterior of the state and model index are obtained recursively through solving the backward-time recursive equations of Bayesian smoothing for linear systems. For this purpose, instead of resorting to methods such as those adopted in [9], [22], the *exact* formula for the quotient of two Gaussian densities [26] is used to evaluate the integral for retrodiction. The only approximation involved in the algorithm development is replacing the smoothed model-matched state posterior, a Gaussian mixture, with a single Gaussian density to achieve computational tractability. 2). Simulation is carried out to evaluate the newly developed technique. We find that the proposed smoothing algorithm has a complexity similar to that of the GPB2-type method [9] but it could accurately approximate the Bayesian optimal solution. Specifically, in the simulated maneuvering target tracking problem, the proposed enhanced smoother performs slightly better than the two-filter approach [16] while being superior to the method from [9].

The rest of this paper is organized as follows. Section II formulates the fixed-interval multiple model smoothing problem in consideration and gives the exact formula for the quotient of two Gaussian densities. Section III presents the enhanced smoothing algorithm and discusses some implementation aspects. Section IV shows the simulation results. Section V concludes the paper.

II. Problem Formulation and the Quotient of Two Gaussian Densities

A. Fixed-Interval Multiple Model Smoothing

Suppose we have collected k measurements $\mathbf{z}_t$, $t = 1, 2, ..., k$, from a dynamic system whose state is going to be identified. At each sampling time t, $\mathbf{z}_t$ is generated using one of the following r linear state-space models[1]

$$\mathbf{x}_t = \mathbf{F}_{t-1}^j \mathbf{x}_{t-1} + \mathbf{v}_{t-1}^j, \tag{1a}$$

$$\mathbf{z}_t = \mathbf{H}_t^j \mathbf{x}_t + \mathbf{w}_t^j, \tag{1b}$$

where $j = 1, 2, ..., r$. $\mathbf{x}_t$ is the system state at time t. $\mathbf{F}_{t-1}^j$ and $\mathbf{H}_j^t$ are the state transition and measurement matrices under model j. $\mathbf{v}_{t-1}^j$ and $\mathbf{w}_t^j$ are the process and measurement noises under model j . They are independent white Gaussian noises with zero mean and covariance $\mathbf{Q}_{t-1}^j$ and $\mathbf{R}_t^j$. That is, $\mathbf{v}_{t-1}^j \sim \mathcal{N}(\mathbf{v}_{t-1}^j; \mathbf{0}, \mathbf{Q}_{t-1}^j)$ and $\mathbf{w}_t^j \sim \mathcal{N}(\mathbf{w}_t^j; \mathbf{0}, \mathbf{R}_t^j)$.

The model switching is assumed to be independent of the process noise. Let M_t^j be the model index indicating that during the time interval $(t-1, t]$, the dynamics of the system can be described using the jth state-space model defined in (1). It evolves according to a homogeneous Markovian jump process with a transition probability matrix $\mathbf{P}$ equal to

$$\mathbf{P}(i, j) = p(M_t^j | M_{t-1}^i) = p_{ij}, \tag{2}$$

[1]But the model index is not known *a priori*.

where $i, j = 1, 2, ..., r$ and $\sum_{j=1}^{M} p_{ij} = 1$.

We are interested in finding the smoothed state posterior $p(\mathbf{x}_t | \mathbf{Z}^k)$ for $t \leq k$ to achieve fixed-interval multiple model smoothing. Here, $\mathbf{Z}^k = \{\mathbf{z}_1, \mathbf{z}_2, ..., \mathbf{z}_k\}$ denotes the set of the measurements obtained within the time window spanning from time 1 to time k.

B. Quotient of Two Gaussian Densities

The quotient of two Gaussian densities can be derived from the product rule of Gaussian density that is given by [26], [27]

$$\mathcal{N}(\mathbf{x}; \boldsymbol{\mu}_a, \boldsymbol{\Sigma}_a) \mathcal{N}(\mathbf{x}; \boldsymbol{\mu}_b, \boldsymbol{\Sigma}_b) = \alpha \cdot \mathcal{N}(\mathbf{x}; \boldsymbol{\mu}_c, \boldsymbol{\Sigma}_c), \tag{3}$$

where

$$\alpha = \mathcal{N}(\boldsymbol{\mu}_a; \boldsymbol{\mu}_b, \boldsymbol{\Sigma}_a + \boldsymbol{\Sigma}_b), \tag{4a}$$

$$\boldsymbol{\Sigma}_c = (\boldsymbol{\Sigma}_a^{-1} + \boldsymbol{\Sigma}_b^{-1})^{-1}, \tag{4b}$$

$$\boldsymbol{\mu}_c = \boldsymbol{\Sigma}_c (\boldsymbol{\Sigma}_a^{-1} \boldsymbol{\mu}_a + \boldsymbol{\Sigma}_b^{-1} \boldsymbol{\mu}_b). \tag{4c}$$

From (3), it is straightforward to write the quotient of two Gaussian densities as

$$\frac{\mathcal{N}(\mathbf{x}; \boldsymbol{\mu}_c, \boldsymbol{\Sigma}_c)}{\mathcal{N}(\mathbf{x}; \boldsymbol{\mu}_a, \boldsymbol{\Sigma}_a)} = \frac{1}{\alpha} \cdot \mathcal{N}(\mathbf{x}; \boldsymbol{\mu}_b, \boldsymbol{\Sigma}_b), \tag{5}$$

where according to (4), we have

$$\boldsymbol{\Sigma}_b = (\boldsymbol{\Sigma}_c^{-1} - \boldsymbol{\Sigma}_a^{-1})^{-1}, \tag{6a}$$

$$\boldsymbol{\mu}_b = \boldsymbol{\Sigma}_b (\boldsymbol{\Sigma}_c^{-1} \boldsymbol{\mu}_c - \boldsymbol{\Sigma}_a^{-1} \boldsymbol{\mu}_a). \tag{6b}$$

To simplifiy the factor $1/\alpha$, we note that

$$\boldsymbol{\Sigma}_a + \boldsymbol{\Sigma}_b = \boldsymbol{\Sigma}_a + (\boldsymbol{\Sigma}_c^{-1} - \boldsymbol{\Sigma}_a^{-1})^{-1} = \boldsymbol{\Sigma}_a (\boldsymbol{\Sigma}_a - \boldsymbol{\Sigma}_c)^{-1} \boldsymbol{\Sigma}_a, \tag{7}$$

$$\begin{aligned} \boldsymbol{\mu}_a - \boldsymbol{\mu}_b &= \boldsymbol{\mu}_a - (\boldsymbol{\Sigma}_c^{-1} - \boldsymbol{\Sigma}_a^{-1})^{-1} (\boldsymbol{\Sigma}_c^{-1} \boldsymbol{\mu}_c - \boldsymbol{\Sigma}_a^{-1} \boldsymbol{\mu}_a) \\ &= (\boldsymbol{\Sigma}_c^{-1} - \boldsymbol{\Sigma}_a^{-1})^{-1} \boldsymbol{\Sigma}_c^{-1} (\boldsymbol{\mu}_a - \boldsymbol{\mu}_c) \\ &= \boldsymbol{\Sigma}_a (\boldsymbol{\Sigma}_a - \boldsymbol{\Sigma}_c)^{-1} (\boldsymbol{\mu}_a - \boldsymbol{\mu}_c). \end{aligned} \tag{8}$$

As a result, $1/\alpha$ can be expressed as

$$\begin{aligned} \beta = 1/\alpha &= 1/\mathcal{N}(\boldsymbol{\mu}_a; \boldsymbol{\mu}_b, \boldsymbol{\Sigma}_a + \boldsymbol{\Sigma}_b) \\ &= \sqrt{|2\pi \boldsymbol{\Sigma}_a (\boldsymbol{\Sigma}_a - \boldsymbol{\Sigma}_c)^{-1} \boldsymbol{\Sigma}_a|} \\ &\quad \times \exp\left(\frac{1}{2} (\boldsymbol{\mu}_a - \boldsymbol{\mu}_c)^T (\boldsymbol{\Sigma}_a - \boldsymbol{\Sigma}_c)^{-1} (\boldsymbol{\mu}_a - \boldsymbol{\mu}_c) \right) \\ &= \frac{|\boldsymbol{\Sigma}_a|}{|\boldsymbol{\Sigma}_a - \boldsymbol{\Sigma}_c|} \cdot \frac{1}{\mathcal{N}(\boldsymbol{\mu}_a; \boldsymbol{\mu}_c, \boldsymbol{\Sigma}_a - \boldsymbol{\Sigma}_c)}. \end{aligned} \tag{9}$$

Inserting (9) into (5) yields the following expression for the quotient of two Gaussian densities[2]

$$\frac{\mathcal{N}(\mathbf{x}; \boldsymbol{\mu}_c, \boldsymbol{\Sigma}_c)}{\mathcal{N}(\mathbf{x}; \boldsymbol{\mu}_a, \boldsymbol{\Sigma}_a)} = \frac{|\boldsymbol{\Sigma}_a|}{|\boldsymbol{\Sigma}_a - \boldsymbol{\Sigma}_c|} \cdot \frac{\mathcal{N}(\mathbf{x}; \boldsymbol{\mu}_b, \boldsymbol{\Sigma}_b)}{\mathcal{N}(\boldsymbol{\mu}_a; \boldsymbol{\mu}_c, \boldsymbol{\Sigma}_a - \boldsymbol{\Sigma}_c)}, \tag{10}$$

which will be utilized in the next section to derive the enhanced fixed-interval multiple model smoother.

[2]Note that (10) is equivalent to but more succint than (C.10) and (C.11) in [26].

III. Proposed Algorithm and Its Implementation

A. Approximating the Bayesian Optimal Smoother

In the multiple model smoothing problem described in Section II, the system state $\mathbf{x}_t$ and model index M_t^j are both unknown. Thus, we shall attempt to calculate the smoothed state posterior $p(\mathbf{x}_t|\mathbf{Z}^k)$ $(t \leq k)$ via first finding the joint posterior $p(\mathbf{x}_t, M_t^j|\mathbf{Z}^k)$ and then marginalizing out M_t^j.

According to the backward-time recursive equations of Bayesian optimal smoothing [3], the desired joint posterior $p(\mathbf{x}_t, M_t^j|\mathbf{Z}^k)$ can be written as [9]

$$p(\mathbf{x}_t, M_t^j|\mathbf{Z}^k) = \sum_{i=1}^{r} \int p(\mathbf{x}_t, M_t^j, \mathbf{x}_{t+1}, M_{t+1}^i|\mathbf{Z}^k)\mathrm{d}\mathbf{x}_{t+1}$$
$$= \sum_{i=1}^{r} \int p(\mathbf{x}_t, M_t^j|\mathbf{x}_{t+1}, M_{t+1}^i, \mathbf{Z}^t)p(\mathbf{x}_{t+1}, M_{t+1}^i|\mathbf{Z}^k)\mathrm{d}\mathbf{x}_{t+1}, \tag{11}$$

where we have, by Bayes theorem,

$$p(\mathbf{x}_t, M_t^j|\mathbf{x}_{t+1}, M_{t+1}^i, \mathbf{Z}^t) = \frac{p(\mathbf{x}_{t+1}, M_{t+1}^i|\mathbf{x}_t, M_t^j)p(\mathbf{x}_t, M_t^j|\mathbf{Z}^t)}{p(\mathbf{x}_{t+1}, M_{t+1}^i|\mathbf{Z}^t)}. \tag{12}$$

The Markov property that the composite vector $[\mathbf{x}_t^T, M_t^j]^T$ would be independent of the measurements collected from time $t+1$ to k given $[\mathbf{x}_{t+1}^T, M_{t+1}^i]^T$ has been applied to establish the second equality in (11).

More importantly, it can be seen that (11) relates the posterior of $[\mathbf{x}_t^T, M_t^j]^T$, $p(\mathbf{x}_t, M_t^j|\mathbf{Z}^k)$, to that of $[\mathbf{x}_{t+1}^T, M_{t+1}^i]^T$, $p(\mathbf{x}_t, M_{t+1}^i|\mathbf{Z}^k)$. This backward-time retrodiction enables the recursive computation of the smoothed joint posterior of the state and model index, which is essential for fixed-interval smoothing. To evaluate (11), we use (1a), (2) and the fact that model index M_t^j is independent of the state to arrive at

$$p(\mathbf{x}_{t+1}, M_{t+1}^i|\mathbf{x}_t, M_t^j) = p(\mathbf{x}_{t+1}|M_{t+1}^i, \mathbf{x}_t)p(M_{t+1}^i|M_t^j)$$
$$= \mathcal{N}(\mathbf{x}_{t+1}; \mathbf{F}_t^i\mathbf{x}_t, \mathbf{Q}_t^i) \cdot p_{ji}. \tag{13}$$

Next, note that $p(\mathbf{x}_t, M_t^j|\mathbf{Z}^t)$ in (12) is the *filtered* joint posterior of the state and model index given measurements up to time t. It can be computed using the forward-time IMM filter (see e.g., [1]) such that it can be expressed as

$$p(\mathbf{x}_t, M_t^j|\mathbf{Z}^t) = p(\mathbf{x}_t|M_t^j, \mathbf{Z}^t)p(M_t^j|\mathbf{Z}^t)$$
$$\approx \mathcal{N}(\mathbf{x}_t; \boldsymbol{\mu}_{t|t}^j, \mathbf{P}_{t|t}^j) \cdot w_{t|t}^j. \tag{14}$$

Here, $p(\mathbf{x}_t|M_t^j, \mathbf{Z}^t)$ is the model-matched state posterior, which is approximated using the single Gaussian density $\mathcal{N}(\mathbf{x}_t; \boldsymbol{\mu}_{t|t}^j, \mathbf{P}_{t|t}^j)$, and $p(M_t^j|\mathbf{Z}^t)$ is the posterior probability of the model index.

Besides, the denominator $p(\mathbf{x}_{t+1}, M_{t+1}^i|\mathbf{Z}^t)$ in (12) is the predicted density of the state and model index. It is calculated in the prediction stage of the forward-time IMM filter, which is equal to

$$p(\mathbf{x}_{t+1}, M_{t+1}^i|\mathbf{Z}^t) = \sum_{l=1}^{r} p_{li} \cdot w_{t|t}^l \cdot \mathcal{N}(\mathbf{x}_{t+1}; \boldsymbol{\mu}_{t+1|t}^{li}, \mathbf{P}_{t+1|t}^{li})$$
$$\approx w_{t+1|t}^i \cdot \mathcal{N}(\mathbf{x}_{t+1}; \boldsymbol{\mu}_{t+1|t}^i, \mathbf{P}_{t+1|t}^i), \tag{15}$$

where $\boldsymbol{\mu}_{t+1|t}^{li} = \mathbf{F}_t^i\boldsymbol{\mu}_{t|t}^l$, $\mathbf{P}_{t+1|t}^{li} = \mathbf{F}_t^i\mathbf{P}_{t|t}^l(\mathbf{F}_t^i)^T + \mathbf{Q}_t^i$, $l = 1, 2, ..., r$, and $w_{t+1|t}^i = \sum_{l=1}^r p_{li} \cdot w_{t|t}^l$. The approximation in (15) is obtained by applying moment matching to replace the Gaussian mixture $\sum_{l=1}^r (p_{li} \cdot w_{t|t}^l / w_{t+1|t}^i) \cdot \mathcal{N}(\mathbf{x}_{t+1}; \boldsymbol{\mu}_{t+1|t}^{li}, \mathbf{P}_{t+1|t}^{li})$ using a single Gaussian density with mean $\boldsymbol{\mu}_{t+1|t}^i$ and covariance $\mathbf{P}_{t+1|t}^i$. This is needed in the forward-time IMM filter to realize model interaction and maintain computational tractability.

Finally, we express $p(\mathbf{x}_{t+1}, M_{t+1}^i|\mathbf{Z}^k)$ in (11) as, by using notations similar to those in (14),

$$p(\mathbf{x}_{t+1}, M_{t+1}^i|\mathbf{Z}^k) = p(\mathbf{x}_{t+1}|M_{t+1}^i, \mathbf{Z}^k)p(M_{t+1}^i|\mathbf{Z}^k)$$
$$\approx \mathcal{N}(\mathbf{x}_{t+1}; \boldsymbol{\mu}_{t+1|k}^i, \mathbf{P}_{t+1|k}^i) \cdot w_{t+1|k}^i. \tag{16}$$

In other words, we shall approximate the smoothed joint posterior of the state and model index for $t \leq k$ using a scaled Gaussian density, as in the forward-time IMM filter. The scaling factor is just the model index probability $w_{t+1|k}^i$, while the Gaussian density $\mathcal{N}(\mathbf{x}_{t+1}; \boldsymbol{\mu}_{t+1|k}^i, \mathbf{P}_{t+1|k}^i)$ is the smoothed model-matched state posterior. This follows from the fact that the backward-time recursion of the Bayesian optimal smoother in (11) would start with $t = k-1$. In this case, $p(\mathbf{x}_{t+1}, M_{t+1}^i|\mathbf{Z}^k)$ becomes equal to $p(\mathbf{x}_k, M_k^i|\mathbf{Z}^k)$, which is the IMM-filtered posterior at time k given in (14). It has the same functional form as (16).

Inserting the results in (12)-(16) into (11), we obtain the following approximation to the backward-time Bayesian optimal smoother as the basis for developing the proposed fixed-interval smoothing algoritm

$$p(\mathbf{x}_t, M_t^j|\mathbf{Z}^k) \approx \sum_{i=1}^{r} \frac{p_{ji} \cdot w_{t|t}^j \cdot w_{t+1|k}^i}{w_{t+1|t}^i}\mathcal{N}(\mathbf{x}_t; \boldsymbol{\mu}_{t|t}^j, \mathbf{P}_{t|t}^j) \times$$
$$\int \frac{\mathcal{N}(\mathbf{x}_{t+1}; \mathbf{F}_t^i\mathbf{x}_t, \mathbf{Q}_t^i)}{\mathcal{N}(\mathbf{x}_{t+1}; \boldsymbol{\mu}_{t+1|t}^i, \mathbf{P}_{t+1|t}^i)}\mathcal{N}(\mathbf{x}_{t+1}; \boldsymbol{\mu}_{t+1|k}^i, \mathbf{P}_{t+1|k}^i)\mathrm{d}\mathbf{x}_{t+1}. \tag{17}$$

In the presence of multiple state-space models, the denominator of the integrand in (17) $\mathcal{N}(\mathbf{x}_{t+1}; \boldsymbol{\mu}_{t+1|t}^i, \mathbf{P}_{t+1|t}^i)$ is not equal to the solution to the Chapman-Kolomogrov equation $\int \mathcal{N}(\mathbf{x}_{t+1}; \mathbf{F}_t^i\mathbf{x}_t, \mathbf{Q}_t^i)\mathcal{N}(\mathbf{x}_t; \boldsymbol{\mu}_{t|t}^j, \mathbf{P}_{t|t}^j)\mathrm{d}\mathbf{x}_t$. This is different from the single model case. Thus, the classic RTS smoother [4] cannot be directly applied to solve the backward-time recursive equation (17) without adopting approximations such as the one in [9] that assumes $\mathbf{P}_{t+1|k}^i \approx \mathbf{O}$ and

$$\mathcal{N}(\mathbf{x}_{t+1}; \boldsymbol{\mu}_{t+1|k}^i, \mathbf{P}_{t+1|k}^i)\mathrm{d}\mathbf{x}_{t+1} \approx \delta(\mathbf{x}_{t+1} - \boldsymbol{\mu}_{t+1|k}^i).$$

Here, $\delta(\cdot)$ is the Dirac delta function.

B. Proposed Fixed-Interval Multiple Model Smoother

We shall evaluate the integral in (17) using the exact formula for the quotient of two Gaussian densities in (10) to develop the proposed fixed-interval multiple model smoother.

The theoretical derivation starts with noting that

$$\frac{\mathcal{N}(\mathbf{x}_{t+1};\mathbf{F}_t^i\mathbf{x}_t,\mathbf{Q}_t^i)}{\mathcal{N}(\mathbf{x}_{t+1};\boldsymbol{\mu}_{t+1|t}^i,\mathbf{P}_{t+1|t}^i)}=a_t^i\cdot\mathcal{N}(\mathbf{x}_{t+1};\boldsymbol{\mu}_{a,t}^i,\boldsymbol{\Sigma}_{a,t}^i), \quad (18)$$

where according to (10), we have

$$\boldsymbol{\Sigma}_{a,t}^i=((\mathbf{Q}_t^i)^{-1}-(\mathbf{P}_{t+1|t}^i)^{-1})^{-1}, \quad (19a)$$
$$\boldsymbol{\mu}_{a,t}^i=\boldsymbol{\Sigma}_{a,t}^i((\mathbf{Q}_t^i)^{-1}\mathbf{F}_t^i\mathbf{x}_t-(\mathbf{P}_{t+1|t}^i)^{-1}\boldsymbol{\mu}_{t+1|t}^i), \quad (19b)$$

and after some straightforward manipulations,

$$a_t^i=\frac{|\mathbf{P}_{t+1|t}^i|\cdot|\mathbf{F}_t^i|}{|\mathbf{P}_{t+1|t}^i-\mathbf{Q}_t^i|}\times \frac{1}{\mathcal{N}(\mathbf{x}_t;(\mathbf{F}_t^i)^{-1}\boldsymbol{\mu}_{t+1|t}^i,(\mathbf{F}_t^i)^{-1}(\mathbf{P}_{t+1|t}^i-\mathbf{Q}_t^i)(\mathbf{F}_t^i)^{-T})}. \quad (20)$$

Substituting (18) into the integral in (17), we can show that the integral is equal to, using the product rule in (3),

$$\int\frac{\mathcal{N}(\mathbf{x}_{t+1};\mathbf{F}_t^i\mathbf{x}_t,\mathbf{Q}_t^i)}{\mathcal{N}(\mathbf{x}_{t+1};\boldsymbol{\mu}_{t+1|t}^i,\mathbf{P}_{t+1|t}^i)}\mathcal{N}(\mathbf{x}_{t+1};\boldsymbol{\mu}_{t+1|k}^i,\mathbf{P}_{t+1|k}^i)\mathrm{d}\mathbf{x}_{t+1} =a_t^i\cdot\mathcal{N}(\mathbf{y}_t^i;\mathbf{G}_t^i\mathbf{x}_t,\boldsymbol{\Sigma}_{a,t}^i+\mathbf{P}_{t+1|k}^i), \quad (21)$$

where

$$\mathbf{y}_t^i=\boldsymbol{\mu}_{t+1|k}^i+\boldsymbol{\Sigma}_{a,t}^i(\mathbf{P}_{t+1|t}^i)^{-1}\boldsymbol{\mu}_{t+1|t}^i, \quad (22a)$$
$$\mathbf{G}_t^i=\boldsymbol{\Sigma}_{a,t}^i(\mathbf{Q}_t^i)^{-1}\mathbf{F}_t^i. \quad (22b)$$

Substituting (18)-(21) into (17) yields

$$p(\mathbf{x}_t,M_t^j|\mathbf{Z}^k)\approx\sum_{i=1}^r\frac{p_{ji}\cdot w_{t|t}^j\cdot w_{t+1|k}^i\cdot|\mathbf{P}_{t+1|t}^i|\cdot|\mathbf{F}_t^i|}{w_{t+1|t}^i\cdot|\mathbf{P}_{t+1|t}^i-\mathbf{Q}_t^i|}\times \frac{\mathcal{N}(\mathbf{y}_t^i;\mathbf{G}_t^i\mathbf{x}_t,\boldsymbol{\Sigma}_{a,t}^i+\mathbf{P}_{t+1|k}^i)\mathcal{N}(\mathbf{x}_t;\boldsymbol{\mu}_{t|t}^j,\mathbf{P}_{t|t}^j)}{\mathcal{N}(\mathbf{x}_t;(\mathbf{F}_t^i)^{-1}\boldsymbol{\mu}_{t+1|t}^i,(\mathbf{F}_t^i)^{-1}(\mathbf{P}_{t+1|t}^i-\mathbf{Q}_t^i)(\mathbf{F}_t^i)^{-T})}. \quad (23)$$

Through invoking the state update stage of the linear Kalman filter [3], the Gaussian product in the numerator of the summand in (23) can be shown to be equal to

$$\mathcal{N}(\mathbf{y}_t^i;\mathbf{G}_t^i\mathbf{x}_t,\boldsymbol{\Sigma}_{a,t}^i+\mathbf{P}_{t+1|k}^i)\mathcal{N}(\mathbf{x}_t;\boldsymbol{\mu}_{t|t}^j,\mathbf{P}_{t|t}^j) =b_t^{ji}\cdot\mathcal{N}(\mathbf{x}_t;\boldsymbol{\mu}_{b,t}^{ji},\boldsymbol{\Sigma}_{b,t}^{ji}), \quad (24)$$

where

$$\boldsymbol{\Sigma}_{b,t}^{ji}=((\mathbf{P}_{t|t}^j)^{-1}+(\mathbf{G}_t^i)^T(\boldsymbol{\Sigma}_{a,t}^i+\mathbf{P}_{t+1|k}^i)^{-1}\mathbf{G}_t^i)^{-1}, \quad (25a)$$
$$\boldsymbol{\mu}_{b,t}^{ji}=\boldsymbol{\Sigma}_b^{ji}((\mathbf{P}_{t|t}^j)^{-1}\boldsymbol{\mu}_{t|t}^j+(\mathbf{G}_t^i)^T(\boldsymbol{\Sigma}_{a,t}^i+\mathbf{P}_{t+1|k}^i)^{-1}\mathbf{y}_t^i), \quad (25b)$$
$$b_t^{ji}=\mathcal{N}(\mathbf{y}_t^i;\mathbf{G}_t^i\boldsymbol{\mu}_{t|t}^j,\mathbf{G}_t^i\mathbf{P}_{t|t}^j(\mathbf{G}_t^i)^T+(\boldsymbol{\Sigma}_{a,t}^i+\mathbf{P}_{t+1|k}^i)). \quad (25c)$$

Putting (24) into (23) and again applying (10), we have

$$\frac{\mathcal{N}(\mathbf{x}_t;\boldsymbol{\mu}_{b,t}^{ji},\boldsymbol{\Sigma}_{b,t}^{ji})}{\mathcal{N}(\mathbf{x}_t;(\mathbf{F}_t^i)^{-1}\boldsymbol{\mu}_{t+1|t}^i,(\mathbf{F}_t^i)^{-1}(\mathbf{P}_{t+1|t}^i-\mathbf{Q}_t^i)(\mathbf{F}_t^i)^{-T})} =c_t^{ji}\cdot\mathcal{N}(\mathbf{x}_t;\boldsymbol{\mu}_{c,t}^{ji},\boldsymbol{\Sigma}_{c,t}^{ji}), \quad (26)$$

where

$$\boldsymbol{\Sigma}_{c,t}^{ji}=((\boldsymbol{\Sigma}_{b,t}^{ji})^{-1}-(\mathbf{F}_t^i)^T(\mathbf{P}_{t+1|t}^i-\mathbf{Q}_t^i)^{-1}\mathbf{F}_t^i)^{-1}, \quad (27a)$$
$$\boldsymbol{\mu}_{c,t}^{ji}=\boldsymbol{\Sigma}_{c,t}^{ji}((\boldsymbol{\Sigma}_{b,t}^{ji})^{-1}\boldsymbol{\mu}_{b,t}^{ji}-(\mathbf{F}_t^i)^T(\mathbf{P}_{t+1|t}^i-\mathbf{Q}_t^i)^{-1}\boldsymbol{\mu}_{t+1|t}^i), \quad (27b)$$

and c_t^{ji} is equal to, after some algebraic manipulations,

$$c_t^{ji}=\frac{|\mathbf{P}_{t+1|t}^i-\mathbf{Q}_t^i|}{|\mathbf{P}_{t+1|t}^i-\mathbf{Q}_t^i-\mathbf{F}_t^i\boldsymbol{\Sigma}_{b,t}^{ji}(\mathbf{F}_t^i)^T|\cdot|\mathbf{F}_t^i|}\times \frac{1}{\mathcal{N}(\boldsymbol{\mu}_{t+1|t}^i;\mathbf{F}_t^i\boldsymbol{\mu}_{b,t}^{ji},\mathbf{P}_{t+1|t}^i-\mathbf{Q}_t^i-\mathbf{F}_t^i\boldsymbol{\Sigma}_{b,t}^{ji}(\mathbf{F}_t^i)^T)}. \quad (28)$$

Using the results from (24) and (26), (23) now becomes

$$p(\mathbf{x}_t,M_t^j|\mathbf{Z}^k)\approx\sum_{i=1}^r d_t^{ji}\cdot\mathcal{N}(\mathbf{x}_t;\boldsymbol{\mu}_{c,t}^{ji},\boldsymbol{\Sigma}_{c,t}^{ji}), \quad (29)$$

where

$$d_t^{ji}=\frac{p_{ji}\cdot w_{t|t}^j\cdot w_{t+1|k}^i\cdot|\mathbf{P}_{t+1|t}^i|}{w_{t+1|t}^i\cdot|\mathbf{P}_{t+1|t}^i-\mathbf{Q}_t^i-\mathbf{F}_t^i\boldsymbol{\Sigma}_{b,t}^{ji}(\mathbf{F}_t^i)^T|}\times \frac{\mathcal{N}(\mathbf{y}_t^i;\mathbf{G}_t^i\boldsymbol{\mu}_{t|t}^j,\mathbf{G}_t^i\mathbf{P}_{t|t}^j(\mathbf{G}_t^i)^T+(\boldsymbol{\Sigma}_{a,t}^i+\mathbf{P}_{t+1|k}^i))}{\mathcal{N}(\boldsymbol{\mu}_{t+1|t}^i;\mathbf{F}_t^i\boldsymbol{\mu}_{b,t}^{ji},\mathbf{P}_{t+1|t}^i-\mathbf{Q}_t^i-\mathbf{F}_t^i\boldsymbol{\Sigma}_{b,t}^{ji}(\mathbf{F}_t^i)^T)}. \quad (30)$$

This completes the development of the proposed fixed-interval multiple model smoother. It is an approximated solution to the backward-time recursive equations of Bayesian optimal smoothing in (11).

To extract the smoothed model-matched state posterior as well as the smoothed posterior probability for the model index from (29), we can factorize $p(\mathbf{x}_t,M_t^j|\mathbf{Z}^k)$ as in (16) into

$$p(\mathbf{x}_t,M_t^j|\mathbf{Z}^k)\approx\mathcal{N}(\mathbf{x}_t;\boldsymbol{\mu}_{t|k}^j,\mathbf{P}_{t|k}^j)\cdot w_{t|k}^j. \quad (31)$$

Comparing it with (29), we have that the smoothed posterior probability for the model index M_t^j is equal to

$$w_{t|k}^j=\frac{\sum_{i=1}^r d_t^{ji}}{\sum_{l=1}^r\sum_{i=1}^r d_t^{li}}. \quad (32)$$

Besides, the mean and covariance of the smoothed model-matched state posterior $p(\mathbf{x}_t|M_t^j,\mathbf{Z}^k)=\mathcal{N}(\mathbf{x}_t;\boldsymbol{\mu}_{t|k}^j,\mathbf{P}_{t|k}^j)$ can be found, using moment matching, to be equal to

$$\boldsymbol{\mu}_{t|k}^j=\frac{1}{\sum_{i=1}^r d_t^{ji}}\sum_{i=1}^r d_t^{ji}\cdot\boldsymbol{\mu}_{c,t}^{ji}, \quad (33a)$$
$$\mathbf{P}_{t|k}^j=\frac{1}{\sum_{i=1}^r d_t^{ji}}\sum_{i=1}^r d_t^{ji}(\boldsymbol{\Sigma}_{c,t}^{ji}+(\boldsymbol{\mu}_{c,t}^{ji}-\boldsymbol{\mu}_{t|k}^j)(\boldsymbol{\mu}_{c,t}^{ji}-\boldsymbol{\mu}_{t|k}^j)^T). \quad (33b)$$

The state posterior $p(\mathbf{x}_t|\mathbf{Z}^k)$ can then be obtained by marginalizing out M_t^j in $p(\mathbf{x}_t, M_t^j|\mathbf{Z}^k)$ through

$$p(\mathbf{x}_t|\mathbf{Z}^k) = \sum_{j=1}^{r} p(\mathbf{x}_t, M_t^j|\mathbf{Z}^k) \approx \sum_{j=1}^{r} \mathcal{N}(\mathbf{x}_t; \boldsymbol{\mu}_{t|k}^j, \mathbf{P}_{t|k}^j) \cdot w_{t|k}^j. \tag{34}$$

Again, the rightmost summation can be evaluated using moment matching to approximate $p(\mathbf{x}_t|\mathbf{Z}^k)$ using a single Gaussian density as the output of the proposed algorithm.

C. Algorithm Summary

With the fixed-interval multiple model smoother developed in the last two subsections, computing the desired smoothed state posterior $p(\mathbf{x}_t|\mathbf{Z}^k)$ can be performed in two stages.

Stage-1: We first begin with the initial model-matched state posterior $p(\mathbf{x}_0|M_0^j) = \mathcal{N}(\mathbf{x}_0; \boldsymbol{\mu}_{0|0}^j, \mathbf{P}_{0|0}^j)$ and initial model index probability $p(M_0^j) = w_{0|0}^j$, where $j = 1, 2, ..., r$. Then, the forward-time IMM filter [1] is applied to the measurements in $\mathbf{Z}^k$ to obtain $p(\mathbf{x}_t|M_t^j, \mathbf{Z}^t) \approx \mathcal{N}(\mathbf{x}_t; \boldsymbol{\mu}_{t|t}^j, \mathbf{P}_{t|t}^j)$ and $p(M_t^j|\mathbf{Z}^t) = w_{t|t}^j$ sequentially for $t = 1, 2, ..., k$.

Stage-2: Next, we start the retrodiction in (29) with $t = k-1$, $p(\mathbf{x}_{t+1}|M_{t+1}^i, \mathbf{Z}^k) \approx \mathcal{N}(\mathbf{x}_{t+1}; \boldsymbol{\mu}_{t+1|k}^i, \mathbf{P}_{t+1|k}^i) = \mathcal{N}(\mathbf{x}_k; \boldsymbol{\mu}_{k|k}^i, \mathbf{P}_{k|k}^i)$ and $p(M_{t+1}^i|\mathbf{Z}^k) = w_{k|k}^i$ found by the forward-time IMM filter at time k, where $i = 1, 2, ..., r$. The obtained smoothed joint posterior $p(\mathbf{x}_t, M_t^j|\mathbf{Z}^k)$ is then inserted into (29) again to compute $p(\mathbf{x}_{t-1}, M_{t-1}^j|\mathbf{Z}^k)$. This process is repeated until $t = 1$. The smoothed state posterior $p(\mathbf{x}_t|\mathbf{Z}^k)$, which is also the algorithm output, is found via (34).

D. Implementation Aspects

At each time $t < k$, the evaluation of (29) can be achieved by carrying out the following four steps in sequence.

- Step-1: calculate $\boldsymbol{\Sigma}_{a,t}^i$ using (19a);
- Step-2: find $\mathbf{y}_t^i$ and $\mathbf{G}_t^i$ using (22);
- Step-3: perform the Kalman update to find $\boldsymbol{\mu}_{b,t}^{ji}$ and $\boldsymbol{\Sigma}_{b,t}^{ji}$ defined in (25a) and (25b);
- Step-4: compute $\boldsymbol{\mu}_{c,t}^{ji}$, $\boldsymbol{\Sigma}_{c,t}^{ji}$ and d_t^{ji} using (27) and (30).

Several remarks on the implementation of the backward-time recursive smoother in (29) are in order.

Remark 1: The proposed smoother requires that the covariance matrices of the process noises in all the r models, $\mathbf{Q}_t^i$, are non-singular. Their inverses are needed when calculating $\boldsymbol{\Sigma}_{a,t}^i$, $\mathbf{y}_t^i$ and $\mathbf{G}_t^i$ (see (19a) and (22)). If $\mathbf{Q}_t^i$ is singular, the method of diagonal loading can be used to achieve invertability. Further improvement of the proposed multiple model smoother to eliminate this constraint is under way.

Remark 2: From (29), we can see that for every model index M_t^j, a total number of r "smoothers" are needed. Therefore, the proposed fixed-interval smoother has a similar complexity as that of the GPB2-type algorithm in [9]. Specifically, both methods requires a total number of r^2 "smoothers" for each backward recursion.

Remark 3: The proposed algorithm involves moment matching-based approximation to replace the Gaussian mixture with a single Gaussian density (see e.g., (15) and (33)). The purpose is to limit the number of Gaussian components used to represent the smoothed state posterior $p(\mathbf{x}_t|M_t^j, \mathbf{Z}^k)$ in order to maintain computational tractability.

Remark 4: When computing $\boldsymbol{\Sigma}_{c,t}^{ji}$ in (27a) using

$$\begin{aligned}\boldsymbol{\Sigma}_{c,t}^{ji} &= ((\boldsymbol{\Sigma}_{b,t}^{ji})^{-1} - (\mathbf{F}_t^i)^T(\mathbf{P}_{t+1|t}^i - \mathbf{Q}_t^i)^{-1}\mathbf{F}_t^i)^{-1} \\ &= \boldsymbol{\Sigma}_{b,t}^{ji} + \boldsymbol{\Sigma}_{b,t}^{ji}(\mathbf{F}_t^i)^T(\mathbf{P}_{t+1|t}^i - \mathbf{Q}_t^i - \mathbf{F}_t^i\boldsymbol{\Sigma}_{b,t}^{ji}(\mathbf{F}_t^i)^T)^{-1}\mathbf{F}_t^i\boldsymbol{\Sigma}_{b,t}^{ji},\end{aligned}$$

we may find that the matrix $\mathbf{P}_{t+1|t}^i - \mathbf{Q}_t^i - \mathbf{F}_t^i\boldsymbol{\Sigma}_{b,t}^{ji}(\mathbf{F}_t^i)^T$ is invertible but no longer positive definite. This would make the Gaussian density in the denominator of d_t^{ji} in (30) invalid.

To address this issue, in this work, we adopt the so-called uncertainty-injection (UI) technique [28], [29] and scale up the covariance $\mathbf{P}_{t+1|t}^i$ as

$$\mathbf{P}_{t+1|t}^i \leftarrow \lambda \cdot \mathbf{P}_{t+1|t}^i, \tag{35}$$

where $\lambda > 1$. In particular, we increase the scaling factor λ until the matrix $\mathbf{P}_{t+1|t}^i - \mathbf{Q}_t^i - \mathbf{F}_t^i\boldsymbol{\Sigma}_{b,t}^{ji}(\mathbf{F}_t^i)^T$ can be factorized using the Cholesky decomposition (i.e., it is now positive definite). Besides, in this case, we compute d_t^{ji} using

$$d_t^{ji} = \frac{p_{ji} \cdot w_{t|t}^j \cdot w_{t+1|k}^i \cdot |\mathbf{P}_{t+1|t}^i|}{w_{t+1|t}^i \cdot |\mathbf{P}_{t+1|t}^i - \mathbf{Q}_t^i - \mathbf{F}_t^i\boldsymbol{\Sigma}_{b,t}^{ji}(\mathbf{F}_t^i)^T|}. \tag{36}$$

We shall justify the effectiveness of the UI technique by examining (19a) and (25a). It can be seen from (25a) that $\boldsymbol{\Sigma}_{b,t}^{ji}$ is also dependent on $\mathbf{P}_{t+1|t}^i$ through $\boldsymbol{\Sigma}_{a,t}^i$. However, scaling up the predictive covariance $\mathbf{P}_{t+1|t}^i$ would not significantly affect $\boldsymbol{\Sigma}_{a,t}^i$. This is because in many practical tracking scenarios, the process noise covariance is generally much smaller than the state prediction covariance (i.e., $\mathbf{P}_{t+1|t}^i \gg \mathbf{Q}_t^i$), which indicates $\boldsymbol{\Sigma}_{a,t}^i \approx \mathbf{Q}_t^i$ (see (19a)). As a result, increasing $\mathbf{P}_{t+1|t}^i$ will not scale up $\boldsymbol{\Sigma}_{b,t}^{ji}$ much but it will make $\mathbf{P}_{t+1|t}^i - \mathbf{Q}_t^i - \mathbf{F}_t^i\boldsymbol{\Sigma}_{b,t}^{ji}(\mathbf{F}_t^i)^T$ positive definite, as desired.

IV. Simulations

This section evaluates the performance of the proposed fixed-interval multiple model smoother in a simulated maneuvering target tracking task. For the purpose of comparison, the foward-time IMM filter [1], two-filter smoother [16] and GPB2-type algorithm developed in [9] are considered as well.

A. Tracking Scenario

The tracking scenario in consideration is similar to the one adopted in [30]. Specifically, a stationary sensor is deployed at the origin to track a point target on the 2-D plane using bearing and range measurements. At time $t = 1$, the target is located at $[234.92\text{km}, 85.50\text{km}]^T$, which is 250km from the sensor. It has an initial velocity of $[-176.8\text{m/s}, -176.8\text{m/s}]^T$.

Denote the target state at time t as $\mathbf{x}_t = [x_t, y_t, \dot{x}_t, \dot{y}_t]^T$, where $[x_t, y_t]^T$ is the target position and $[\dot{x}_t, \dot{y}_t]^T$ is the target velocity. The target motion is governed by either the constant velocity (CV) model [7]

$$\mathbf{x}_t = \mathbf{F}\mathbf{x}_{t-1} + \mathbf{v}_{t-1}, \tag{37}$$

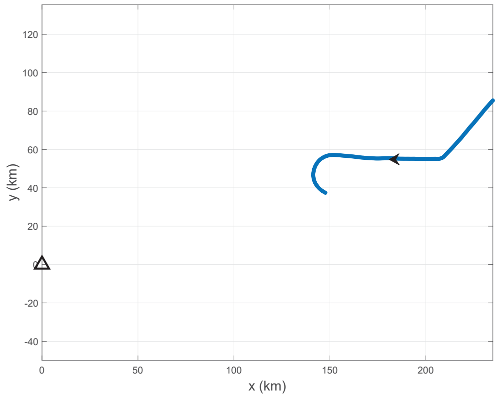

Fig. 1. The considered 2-D maneuvering target tracking scenario. The triangle symbol denotes the sensor.

or the constant turn (CT) model [7]

$$\mathbf{x}_t = \mathbf{F}(\omega) \cdot \mathbf{x}_{t-1} + \mathbf{v}_{t-1}. \tag{38}$$

In the CV model, the state transition matrix $\mathbf{F}$ is equal to

$$\mathbf{F} = \begin{bmatrix} 1 & T \\ 0 & 1 \end{bmatrix} \otimes \mathbf{I}_2, \tag{39}$$

and $\otimes$ is the Kronecker product. In the CT model, ω is the turn rate and the state transition matrix $\mathbf{F}(w)$ is

$$\mathbf{F}(\omega) = \begin{bmatrix} 1 & 0 & \sin(\omega T)/\omega & -(1-\cos(\omega T))/\omega \\ 0 & 1 & (1-\cos(\omega T))/\omega & \sin(\omega T)/\omega \\ 0 & 0 & \cos(\omega T) & -\sin(\omega T) \\ 0 & 0 & \sin(\omega T) & \cos(\omega T) \end{bmatrix}. \tag{40}$$

The system sampling period is $T = 3$s. The process noise $\mathbf{v}_{t-1}$ in the CV model and CT model is Gaussian. It has zero mean and a covariance $\mathbf{Q}_{t-1}$ equal to

$$\mathbf{Q}_{t-1} = \sigma_v^2 \mathbf{G}_{t-1} \mathbf{G}_{t-1}^T + \begin{bmatrix} T^2 \mathbf{I}_2 & \mathbf{O} \\ \mathbf{O} & \mathbf{O} \end{bmatrix}, \tag{41}$$

where the gain matrix is $\mathbf{G}_{t-1} = [T^2/2, T]^T \otimes \mathbf{I}_2$ and $\sigma_v = 1$m/s. The first term on the right hand side of (41) is due to the presence of random acceleration, while the second term comes from the random target position jittering. It can be verified that $\mathbf{Q}_{t-1}$ is invertible. In the simulation, all the smoothing algorithms considered use the *same* process noise covariance.

Consider a time window of 600s. Within the time window, the target performs two turns and they have fixed but different turn rates. The first turn has an acceleration of 1g and a turn rate of $\omega = -0.05$rad/s. It starts at 200s and ends at 218s. The second turn begins at 480s and continues until 600s. It has an acceleration of 0.5g and a turn rate of $\omega = 0.022$rad/s. During other time segments in the time window, the target's motion follows the CV model in (37).

At each sampling time, the stationary sensor at the origin obtains one bearing and one range measurements. They are related to the target state $\mathbf{x}_t$ via

$$\mathbf{y}_t = \begin{bmatrix} \sqrt{x_t^2 + y_t^2} \\ \arctan(x_t/y_t) \end{bmatrix} + \mathbf{w}_t. \tag{42}$$

$\mathbf{w}_t$ is the measurement noise. It is also white Gaussian with zero mean and covariance $\mathbf{R} = \text{diag}(\sigma_r^2, \sigma_\theta^2)$, where $\sigma_r = 50$m and $\sigma_\theta = 0.5^o$.

The four algorithms in consideration, namely the forward-time IMM filter [1], the GPB2-type method from [9], the two-filter smoother [16] and the proposed enhanced smoothing technique, all employ the same set of $r = 7$ state-space models to tackle the target maneuvering. The measurement equation for these state-space models is given in (42). Their process equations are specified by (38) with their turn rates being equal to 0, $\pm$0.1rad/s, $\pm$0.033rad/s and $\pm$0.02rad/s. Note that when the turn rate ω is 0, the CT model in (38) reduces to the CV model defined in (37). In other words, the set of candidate state-space models used by the filtering and smoothing algorithms consists of one CV model and six CT models with different turn rates.

We initialize the forward-time IMM filter using the bearing and range measurements obtained at time $t = 1$. In particular, we set $[x_1, y_1]^T$ to be the target position estimate $[r_1 \sin(\theta_1), r_1 \cos(\theta_1)]^T$, whose covariance is

$$\mathbf{J}_1 \approx \begin{bmatrix} \sin(\theta_1) & r_1 \cos(\theta_1) \\ \cos(\theta_1) & -r_1 \sin(\theta_1) \end{bmatrix} \mathbf{R} \begin{bmatrix} \sin(\theta_1) & r_1 \cos(\theta_1) \\ \cos(\theta_1) & -r_1 \sin(\theta_1) \end{bmatrix}^T. \tag{43}$$

We set the target velocity estimate at time $t = 1$ to be $[0, 0]^T$. As a result, the covariance for the estimate of the true target state $\mathbf{x}_1$, $\mathbf{x}_{1|1} = [r_1 \sin(\theta_1), r_1 \cos(\theta_1), 0, 0]^T$, would be

$$\mathbf{P}_{1|1} = \begin{bmatrix} \mathbf{J}_1 & \mathbf{O} \\ \mathbf{O} & v_{max}^2 \mathbf{I}_2 \end{bmatrix}, \tag{44}$$

where $v_{max} = 250$m/s specifies the maximum possible target speed. All the $r = 7$ models have the same initial state estimate, state covariance and initial model probabilities at time $t = 1$, which is equal to $1/7$. The model transition probability matrix $\mathbf{P}$ have its diagonal elements equal to 0.8 and its off-diagonal elements equal to 0.033.

The filtering results of the forward-time IMM filter are *shared* among the three smoothers simulated for fair comparison. Besides, when implementing the forward-time IMM filter and two-filter smoother, the cubature Kalman filter (CKF) [31] is applied to perform state update and model-matched measurement likelihood calculation.

B. Results

In the experiment, 1000 Monte Carlo runs are performed. In Figs. 2 and 3, we plot, as a function of time, the estimation root mean square errors (RMSEs) for the target position and velocity from the four algorithms in consideration. To facilitate the comparison, the forward-time IMM filter [1] is denoted by 'IMM Filter', the two-filter smoother [16] is denoted by 'Two-filter' and the GPB2-type smoother [9] is denoted by 'GPB2'. Three vertical lines are included in the figures to show the starting time of the first turn, ending time of the first turn and starting time of the second turn, respectively.

It can be seen from Figs. 2 and 3 that as expected, all the smoothers outperform in terms of significantly reduced estimation RMSEs over the forward-time IMM filter. But the GPB2-type smoother exhibits large variation in its position estimation RMSE, due to the use of the assumption that the smoothed state estimates are noise-free but in fact, they have errors (see discussions under (17)). The proposed multiple model smoother offers evidently improved position estimation performance over the GPB2-type smoother, probably due to it using fewer approximations. Compared with the two-filter approach, it provides slightly enhanced performance in identifying both the target position and velocity.

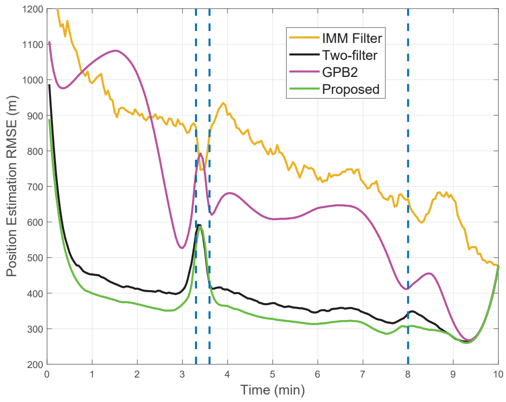

Fig. 2. Comparison of target position RMSEs.

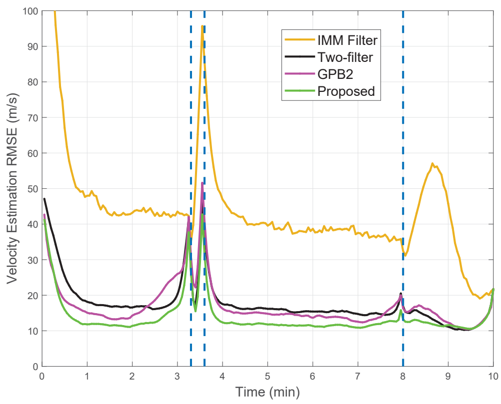

Fig. 3. Comparison of target velocity RMSEs.

To gain more insights, we plot the posterior probability of model index M_t^j as a function of time for the CV model (Fig. 4), CT model with turn rate $w = 0.02$rad/s (Fig. 5) and CT model with $w = -0.033$rad/s (Fig. 6). The results are from a particular Monte Carlo run.

Fig. 4 shows that from 0s to 200s and from 218s to 480s when the target motion follows the CV model, the posterior

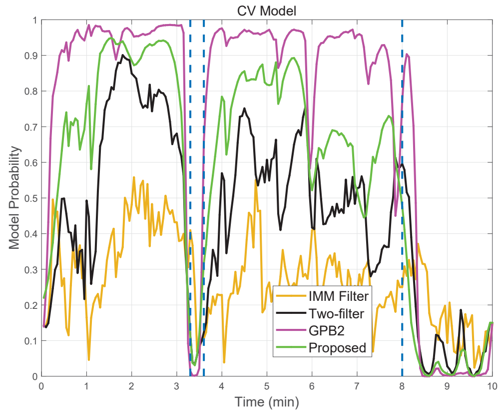

Fig. 4. Comparison of the CV model probability ($\omega = 0$rad/s).

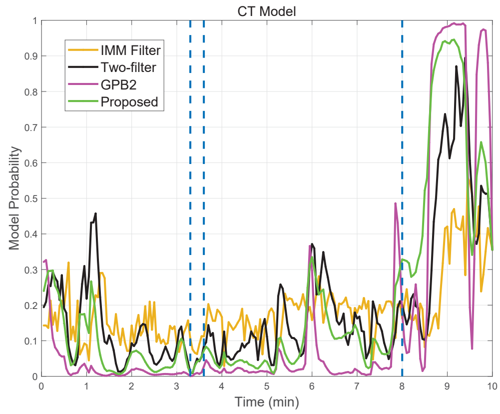

Fig. 5. Comparison of the CT model probability ($\omega = 0.02$rad/s).

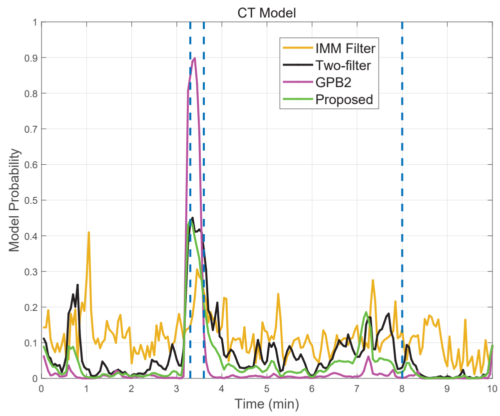

Fig. 6. Comparison of the CT model probability ($\omega = -0.033$rad/s).

probability of the corresponding model index found by the proposed smoother is generally larger than those from the two-filter algorithm and the IMM filter. This indicates that the proposed smoother better matches the target motion pattern within this time period, which leads to improved tracking accuracy observed in Figs. 2 and 3. On the other hand, the posterior model index probability calculated by the GPB2-type method exhibits large variations over time. This may degrade the tracking performance as shown in Fig. 2.

The *assumed* turn rates of the two CT models considered here are very close to the true target turn rates during (480s, 600s) and (200s, 218s). By examining Figs. 5 and 6 that show the posterior probability of their model indices over time, observations very similar to those from Fig. 4 can be obtained. The proposed smoother performs well in correctly identifying the target motion model.

V. Conclusions

This paper presented an enhanced multiple model smoother for Markovian switching systems. Its development relies on solving the smoothing problem by jointly estimating the posterior of the system state and model index, and applying the exact formula for the quotient of two Gaussian densities. The developed algorithm consists of a forward-time IMM filter to achieve state filtering and an approximated solution to the recursive equations of the Bayesian optimal smoother to attain state smoothing. The only approximation required to establish the proposed algorithm is to replace the model-matched posterior, which is a Gaussian mixture, with a single Gaussian density found by moment matching. This makes the new algorithm perform as good as, if not better than, several other smoothers in tracking a maneuvering target.

As future work, we shall generalize the developed method to the case where the state transition is governed by nonlinear functions (cf. (1a)). Besides, investigating its performance in the time difference of arrival (TDOA) and frequency difference of arrival (FDOA)-based target tracking [32] is in progress.

References

[1] Y. Bar-Shalom, X. R. Li, and T. Kirubarajan, *Estimation with applications to tracking and navigation: Theory, algorithms and software*. New York: Wiley, 2001.

[2] S. Challa, M. R. Morelande, D. Mus̆icki, and R. J. Evans, *Fundamentals of Object Tracking*. Cambridge University Press, 2011.

[3] S. Särkkä, *Bayesian Filtering and Smoothing*. New York: Cambridge University Press, 2013.

[4] H. Rauch, F. Tung, and C. Striebel, "Maximum likelihood estimates of linear dynamic systems," *AIAA Journal*, vol. 3, pp. 1445–1450, Aug. 1965.

[5] H. Ohlsson, F. Gustafsson, L. Ljung, and S. Boyd, "State smoothing by sum-of-norms regularization," in *Proc. IEEE Conf. Decision and Control (CDC)*, Atlanta, GA, USA, Dec. 2010.

[6] ——, "Smoothed state estimates under abrupt changes using sum-of-norms regularization," *Automatica*, vol. 48, pp. 595–605, Aug. 2012.

[7] X. R. Li and V. P. Jilkov, "Survey of maneuvering target tracking. Part I. Dynamic models," *IEEE Trans. Aerosp. Electron. Syst.*, vol. 39, pp. 1333–1364, Oct. 2003.

[8] ——, "Survey of maneuvering target tracking. Part V. Multiple-model methods," *IEEE Trans. Aerosp. Electron. Syst.*, vol. 41, pp. 1255–1321, Oct. 2005.

[9] W. Koch, "Fixed interval retrodiction approach to Bayesian IMM-MHT for maneuvering multiple targets," *IEEE Trans. Aerosp. Electron. Syst.*, vol. 36, pp. 2–14, Jan. 2000.

[10] Z. Li and H. Leung, "An expectation maximization-based simultaneous registration and fusion algorithm for radar networks," in *Proc. Canadian Conf. on Electrical and Computer Engineering (CCECE)*, Ottawa, ON, Canada, May 2006.

[11] İ. Özbek, M. Hasegawa-Johson, and M. Demirekler, "On improving dynamic state space approaches to articulatory inversion with MAP based parameter estimation," *IEEE Trans. Audio, Speech and Language Process.*, vol. 20, pp. 67–81, Jan. 2012.

[12] V. P. Jilkov, X. R. Li, and L. Lu, "Performance enhancement of the IMM estimation by smoothing," in *Proc. Int. Conf. Inf. Fusion (FUSION)*, Annapolis, MD, USA, Jul. 2002, pp. 713–720.

[13] M. Malleswaran, V. Vaidehi, S. Irwin, and B. Robin, "IMM-UKF-TFS model-based approach for intelligent navigation," *The Journal of Navigation*, vol. 66, pp. 859–877, Nov. 2013.

[14] W. Ali, Y. Li, M. Raja, and N. Ahmed, "Generalized pseudo Bayesian algorithms for tracking of multiple model underwater maneuvering target," *Applied Acoustics*, vol. 166, pp. 1–11, Sept. 2020.

[15] J. García, J. A. Besada, J. M. Molina, and G. de Miguel, "Model-based trajectory reconstruction with IMM smoothing and segmentation," *Information Fusion*, vol. 22, pp. 127–140, March 2015.

[16] R. Helmick, W. Blair, and S. Hoffman, "Fixed-interval smoothing for Markovian switching systems," *IEEE Trans. Inf. Theory*, vol. 41, pp. 1845–1855, June 1995.

[17] D. C. Fraser and J. E. Potter, "The optimal linear smoother as a combination of two optimum linear filters," *IEEE Trans. Automatic Control*, vol. 14, pp. 387–390, August 1969.

[18] D. Q. Mayne, "A solution to the smoothing problem for linear dynamic systems," *Automatica*, vol. 4, pp. 73–92, December 1966.

[19] M. Briers, A. Doucet, and S. Maskell, "Smoothing algorithms for state-space models," *Annals of the Institute of Statistcal Mathematics*, vol. 62, pp. 61–89, 2010.

[20] B. Chen and J. K. Tugnait, "Interacting multiple model fixed-lag smoothing algorithm for Markovian switching systems," *IEEE Trans. Aerosp. Electron. Syst.*, vol. 36, pp. 243–250, Jan. 2000.

[21] N. Nadarajah, R. Tharmarasa, M. McDonald, and T. Kirubarajan, "IMM forward filtering and backward smoothing for manuevering target tracking," *IEEE Trans. Aerosp. Electron. Syst.*, vol. 48, pp. 2673–2678, July 2012.

[22] R. Lopez and P. Danès, "Low-complexity IMM smoothing for jump Markov nonlinear systems," *IEEE Trans. Aerosp. Electron. Syst.*, vol. 53, pp. 1261–1272, June 2017.

[23] ——, "Exploiting Rauch-Tung-Striebel formulae for IMM-based smoothing of Markovian switching systems," in *Proc. IEEE Int. Conf. Acoustics, Speech and Signal Process. (ICASSP)*, Kyoto, Japan, March 2012, pp. 3953–3956.

[24] ——, "A fixed-interval smoother with reduced complexity for jump Markov nonlinear systems," in *Proc. Int. Conf. Inf. Fusion (FUSION)*, Salamanca, Spain, Jul. 2014, pp. 1–8.

[25] Y. Yang, Y. Qin, Y. Yang, Q. Pan, and Z. Li, "A Gaussian mixture smoother for Markovian jump linear systems with non-Gaussian noises," in *Proc. Int. Conf. Inf. Fusion (FUSION)*, Cambridge, UK, Jul. 2018, pp. 2564–2571.

[26] J. M. Hernández-Lobato, "Balancing flexibility and robustness in machine learning: Semiparametric methods and sparse linear models," Ph.D. dissertation, Universidad Autónoma de Madrid, 2010.

[27] D. Acar and U. Orguner, "Information decorrelation for an interacting multiple model filter," in *Proc. Intl. Conf. Information Fusion (FUSION)*, Cambridge, UK, July 2018, pp. 1527–1534.

[28] S. V. Vaerenbergh, M. Lázaro-Gredilla, and I. Santamaría, "Kernel recursive least-squares tracker for time-varying regression," *IEEE Trans. Neural Networks and Learning Systems*, vol. 23, pp. 1313–1326, August 2012.

[29] L. Yang, K. Wang, and L. S. Mihaylova, "Online sparse multi-output Gaussian process regression and learning," *IEEE Trans. Signal and Info. Process. over Networks*, vol. 5, pp. 258–272, June 2019.

[30] X. Li, Y. Liu, L. S. Mihaylova, L. Yang, S. Weddell, and F. Guo, "Enhanced multiple model GPB2 filtering using variational inference," in *Proc. Intl. Conf. Information Fusion (FUSION)*, Ottawa, ON, Canada, July 2019, pp. 2572–2579.

[31] I. Arasaratnam and S. Haykin, "Cubature Kalman filters," *IEEE Trans. Autom. Control*, vol. 54, no. 6, pp. 1254–1269, Jun. 2009.

[32] X. Li, L. Yang, L. S. Mihaylova, F. Guo, and M. Zhang, "Enhanced GMM-based filtering with measurement update ordering and innovation-based pruning," in *Proc. Intl. Conf. Information Fusion (FUSION)*, Cambridge, UK, July 2018, pp. 2572–2579.